mathematics

MDPI

Article

Inverse Inference of Component Reliability for *k*-Out-of-*n* Systems Based on Maximum Entropy and Hazard-Rate Matrix Representation

Chao Li [1,†], Tianci Gong [2,†], Daoqing Zhou [3], Jingjing He [4] and Xuefei Guan [2,*]

[1] AECC Hunan Aviation Powerplant Research Institute, Zhuzhou 412002, China
[2] Graduate School of China Academy of Engineering Physics, Beijing 100193, China
[3] China North Engine Research Institute, Tianjin 300400, China
[4] School of Reliability and Systems Engineering, Beihang University, Beijing 100191, China
* Correspondence: xfguan@gscaep.ac.cn
† These authors contributed equally to this work.

Abstract

This study presents a rational inverse inference framework for *k*-out-of-*n* systems that derives component-level reliability characteristics from system-level failure and monitoring data. The framework employs a hazard-rate matrix to represent the degradation hierarchy and applies the principle of maximum entropy to allocate system-level probabilities to latent component-state configurations without bias, yielding analytical solutions for component hazard rates. The key innovation lies in combining maximum entropy with the hazard-rate matrix, which overcomes the ill-posed nature of the inverse problem and enables systematic integration of heterogeneous auxiliary information within a unified formulation, including system-level multi-state observations, component-wise moment constraints, sub-component data, and inter-component dependencies. This flexibility addresses a major limitation of existing inverse methods, such as Bayesian approaches, which are typically restricted to a single data type and often require strong prior assumptions or extensive failure datasets. The practical applicability of the framework is demonstrated through a case study of a west-to-east gas pipeline pumping system, highlighting its effectiveness in processing multiple information types and delivering actionable component-level reliability assessments for maintenance decision support. To the best of our knowledge, this is the first study to formulate and solve the inverse inference problem for *k*-out-of-*n* systems in a theoretically grounded and information-theoretically optimal manner.

Keywords: *k*-out-of-*n* system; inverse inference; output only; maximum entropy principle; hazard-rate matrix

MSC: 60K20; 62N05

Received: 28 February 2026
Revised: 27 March 2026
Accepted: 31 March 2026
Published: 1 April 2026

1. Introduction

The *k*-out-of-*n* model is widely used in reliability analysis for a variety of complex engineering systems [1]. A *k*-out-of-*n*:*F* system is defined as a system of *n* components whose failure occurs when a total of *k* components have failed [2,3]. A parallel definition exists for the *k*-out-of-*n*:*G* system, which is operable only when at least *k* components are functioning simultaneously. The two formulations are closely related and can be used interchangeably under certain conditions [3]; therefore, the *k*-out-of-*n*:*F* system, or for short

k-out-of-*n*, is considered hereafter in this study. The series and parallel reliability models are special cases of the *k*-out-of-*n* system. For example, a series model corresponds to a 1-out-of-*n* system, while a parallel model corresponds to an *n*-out-of-*n* system [4].

The reliability analysis of *k*-out-of-*n* systems was first explicitly mentioned and discussed by Birnbaum et al. [2] in the early 1960s. However, the mathematical foundations underlying such systems can be traced to the early 1950s, when Moore and Shannon developed a systematic framework for constructing reliable circuits from less reliable relays [5]. This work, partially inspired by von Neumann [6], was subsequently extended in several theoretical generalizations [7,8]. Although not the primary focus of those studies, the *k*-out-of-*n* system can be viewed as a special case of a two-terminal network comprising *n* relays, which is considered closed when at least *k* relays have their contacts closed. In this context, the set of all paths connecting the two terminals that render the circuit closed collectively defines the operable states of the network. Since then, the *k*-out-of-*n* reliability model has been extended to accommodate a wide range of application-oriented requirements. Notable examples include models with repairable components subject to random [9] or general [10] repair times, components with different weight [11–14], dynamic component partnerships [15], correlated failures [16], continuous-review repair parts policies [17], and limited spares and repair capacity [18,19]. Further developments include consecutive *k*-out-of-*n* systems [20–22] and their variants [23–25], along with various evaluation methods [26–29], among many others [30–36]. Combined with exact and/or asymptotic computational techniques, these studies predominantly address the forward problem in system reliability, namely, evaluating system reliability given component-level reliability information.

The inverse problem in a *k*-out-of-*n* system, by contrast, concerns the inference of component-level reliability from system-level observation data. This problem arises in a wide range of practical scenarios, for example, in systems lacking diagnostic units, in cases where diagnostic units fail first, or in efforts to identify the most vulnerable component among heterogeneous components. This type of inverse inference is also related to a broader set of engineering reconstruction problems, where latent structural or component-level information is recovered from incomplete or indirect observations, such as in structural response reconstruction, wavefield reconstruction, flaw imaging, and information demodulation [37–40]. However, this inverse problem remains insufficiently studied in the context of *k*-out-of-*n* systems. Existing methods generally lack a theoretically grounded framework that can overcome the ill-posedness of the inverse problem while systematically incorporating heterogeneous auxiliary information. In parallel, moment-based quadrature methods have shown strong potential in uncertainty quantification, sensitivity analysis, and reliability assessment under limited information, which further motivates the incorporation of moment constraints in the present framework [41–43]. Therefore, the objective of this study is to develop a rational inverse inference framework for *k*-out-of-*n* systems that transforms system-level observations into component-level reliability characteristics in an analytically tractable and unbiased manner. The main contributions of this work are summarized as follows. (1) A rational inverse inference framework is proposed to derive component-level failure characteristics from system-level observations. By employing the hazard-rate matrix as a structured descriptor of the degradation hierarchy, the framework combines it with the principle of maximum entropy (MaxEnt) to allocate system-level probabilities to latent component-state configurations without bias. This formulation overcomes the ill-posed nature of the inverse problem and yields analytical solutions for component hazard rates without relying on arbitrary assumptions. (2) The proposed framework can integrate heterogeneous information types within a unified formulation. It accommodates system-level multi-state observations, inter-

component dependencies, sub-component data, and component-wise moment information. Inter-component correlations are naturally encoded in the off-diagonal entries of the hazard-rate matrix, while sub-component information is incorporated by expanding each diagonal entry into a component-level sub-matrix. Moment information is introduced as constraints in the MaxEnt optimization. This flexibility overcomes an important limitation of existing inverse methods, such as Bayesian approaches, which typically handle only a single type of data and often require strong prior assumptions or extensive failure datasets. (3) The practical applicability of the framework is demonstrated through a long-distance pipeline pumping system case study. The results show the effectiveness of the proposed method in processing multiple information types and delivering actionable component-level reliability assessments for maintenance decision support.

The remainder of this study is organized as follows. First, the mathematical description of the k-out-of-n system is presented, the corresponding inverse inference problem is defined, and the types of information that can be handled within the proposed framework are briefly discussed. The required theoretical tools, such as the hazard-rate matrix and the MaxEnt principle, are also introduced. Next, the inverse inference framework is developed, and the derivations and theoretical solutions for fusing different information sources are provided. Following that, a case study of a west-to-east gas pipeline monitoring system is presented to demonstrate the practical applicability. Finally, conclusions and future research directions are given.

2. Problem Formulation and Preliminaries

To motivate the discussion, the system considered in this study is abstracted as a k-out-of-n structure, and $\mathbb{S}$ denotes the finite set of observable system states. Depending on the cardinality of $\mathbb{S}$, two types of systems are considered.

For systems whose observable states are limited to failure or survival, the state space is binary, i.e., $\mathbb{S} = \{0, 1\}$, where 0 and 1 represent the failure and survival states, respectively. A typical example of a binary-state system is a redundant relay circuit, where the system outcome is either open or closed. In contrast, multi-state systems are those in which the observable state is either a continuous variable or a set of discrete values. Representative examples include network routing systems composed of multiple routers and water pipeline systems driven by a series of pumps. In such systems, the failure of partial components such as routers and pumps may reduce throughput or flow rate, while the system may still operate at a degraded level. Accordingly, the system output can be normalized with respect to its design value to the range $[0, 1]$. Specifically, it equals 1 when all components function properly and 0 when all components fail. In this case, the finite set of observable states is denoted $\mathbb{S} = \{q_c\}$, where $0 \leq q_c \leq 1$, and c indexes the observable states.

Let S_i denote the set of actual states of a k-out-of-n system when exactly i components fail, and let S_{ij} be the j-th n-tuple element of S_i. As an illustration, consider the case of three components with a single failure. The set S_1 is then given by $S_1 = \{S_{11}, S_{12}, S_{13}\}$, where $S_{11} = (0, 1, 1)$, $S_{12} = (1, 0, 1)$, and $S_{13} = (1, 1, 0)$. Each 3-tuple represents the joint state (failure/survival) of the individual components. The cardinality of S_i in this case is the binomial coefficient $|S_i| = C_n^i = \binom{n}{i}$. For a k-out-of-n system, $\{S_0, S_1, \ldots, S_{k-1}\}$ constitutes the set of system states corresponding to survival, whereas $\{S_k, S_{k+1}, \ldots, S_n\}$ corresponds to system failure.

For a k-out-of-n system whose components share an identical reliability function $R(t)$, the system reliability, i.e., $\Pr(\mathbb{S} = 1)$, at time t is written as

$$R_S(t) = \sum_{i=0}^{k-1} C_n^i \cdot [1 - R(t)]^i [R(t)]^{n-i}, \tag{1}$$

where $R_S(t)$ is the reliability function of the system. Without assuming that all components have an identical reliability function, the system reliability at time t can be compactly expressed as

$$R_S(t) = \sum_{i=0}^{k-1} \left[\sum_{j=1}^{C_n^i} \left(\prod_{u=1}^{n} [F_u(t)]^{1-S_{ij}[u]} [R_u(t)]^{S_{ij}[u]} \right) \right], \tag{2}$$

where S_{ij} is defined as above, $S_{ij}[u]$ denotes the u-th element of the n-tuple S_{ij}, $F_u(t) = 1 - R_u(t)$, and $R_u(t)$ is the reliability function of the u-th component. For instance, for a two-out-of-three system, i.e., $k = 2,\ n = 3$, $S_1 = \{S_{11}, S_{12}, S_{13}\} = \{(0,1,1), (1,0,1), (1,1,0)\}$ and $S_{11}[1] = 0,\ S_{11}[2] = 1,\ S_{11}[3] = 1$. In this case, Equation (2) expands to

$$\begin{aligned} R_S(t) &= \sum_{j=1}^{C_3^0} \left(\prod_{u=1}^{3} [F_u(t)]^{1-S_{0j}[u]} [R_u(t)]^{S_{0j}[u]} \right) + \sum_{j=1}^{C_3^1} \left(\prod_{u=1}^{3} [F_u(t)]^{1-S_{1j}[u]} [R_u(t)]^{S_{1j}[u]} \right) \\ &= R_1(t)R_2(t)R_3(t) + F_1(t)R_2(t)R_3(t) + R_1(t)F_2(t)R_3(t) + R_1(t)R_2(t)F_3(t). \end{aligned} \tag{3}$$

Equation (2) provides a general expression for the reliability function of a k-out-of-n system. With the knowledge of the component reliability functions $R_u(t)$ for $u = 1, 2, \ldots, n$, the system reliability $R_S(t)$ can be readily evaluated, corresponding to the forward problem discussed before. In inverse inference, however, the number of unknowns on the right-hand side of Equation (2) typically exceeds the number of observable variables, since $n > 1$ in practical k-out-of-n systems, rendering the problem ill-posed. To address this issue, relevant and appropriate constraints must be incorporated. The construction of such constraints reflects a principled use of available information, as discussed next.

2.1. Date and Information for Inverse Inference

Building on the above description, the inverse problem can be reframed as computing the hazard rates of components in a k-out-of-n system from various types of testable information. Here, testable information refers to information for which, given a candidate component hazard rate, there exists a verifiable procedure to determine whether that hazard rate is consistent with the information [44].

2.1.1. Direct System-Level State Observations

Direct observations of the system state as a function of time for binary-state systems and multi-state systems are illustrated in Figure 1a and Figure 1b, respectively. Such data can be converted into testable information at the system level through standard statistical modeling. For a binary-state system, the observed switching time t is a realization of the random variable T, representing the failure time or lifetime of the system. Given observations from multiple independent and identically operated systems, the system lifetime distribution can be established using probabilistic methods. For a multi-state system, the observation consists of a sequence of state transitions over time. The observed vector $\boldsymbol{t} = (t_1, t_2, \ldots, t_k)$ is a realization of the random vector $\boldsymbol{T} = (T_1, T_2, \ldots, T_k)$, where T_i denotes the time at which the system changes from one observable state to the next during the evolution from complete health to final failure. Using observations collected from multiple independent systems, the discrete probability distribution of the system being in one of the observable states can be obtained.

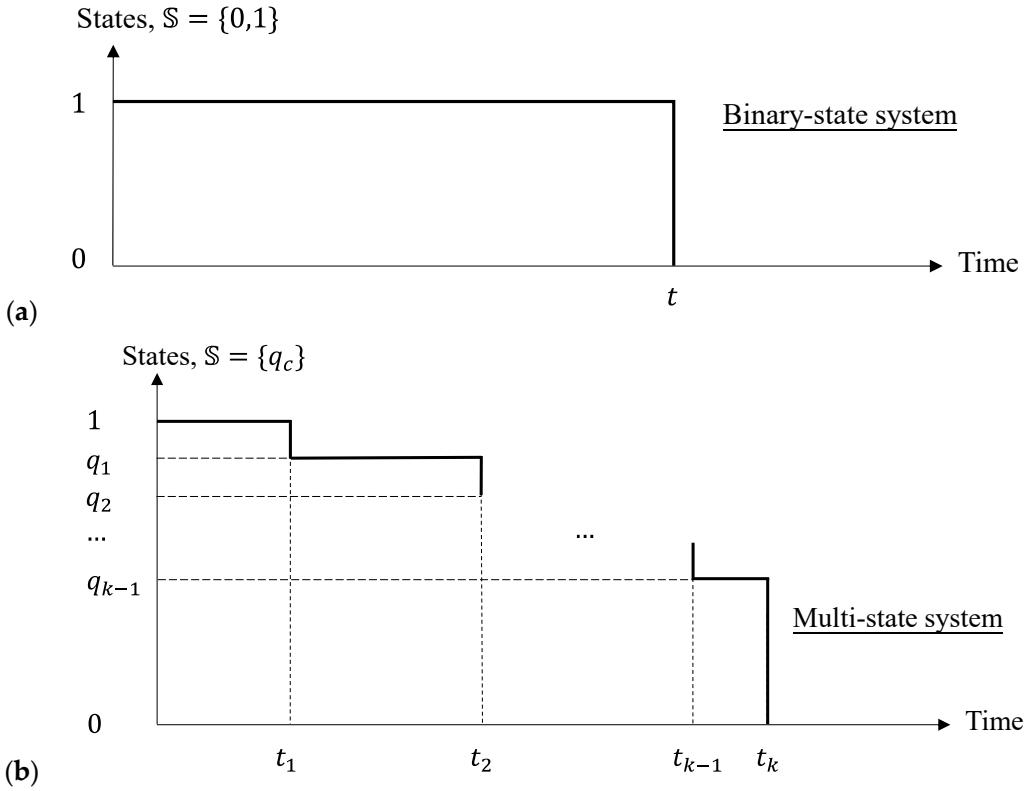

Figure 1. Observed state vs. time data for (**a**) a binary-state system and (**b**) a multi-state system.

In a multi-state system, the numerical values of observable states are inherently context-dependent. For instance, consider a long-range pipeline supply system driven by multiple pumps connected in series. Following the failure of one or more pumps, the delivered volume per unit time decreases; nevertheless, the system may remain operational provided the number of failed pumps does not exceed a critical threshold necessary for maintaining sufficient transport power. The system output, and therefore the observable state, can thus assume multiple levels determined by the joint health status of the individual pumps. Notably, the number of observable output levels, i.e., the number of values on the y-axis in Figure 1b, need not equal the total number of actual component-configuration states, as distinct failure configurations may yield an identical observed output. For example, any two failed pumps could result in the same outlet flow rate, despite the number of distinct configurations being $|S_2| = C_n^2$. Furthermore, output degradation is not necessarily linear in the number of failed components; a failure of one-quarter of the pumps, for instance, does not imply a 25% reduction in output. In practice, the mapping from the number or configuration of failed components to the observed output can be established through physics-based modeling or controlled experiments.

From a statistical perspective, the state-time data are collected to estimate the system-level probabilistic measure of the observable state without requiring explicit knowledge of the system structure, as the target of interest is the probability law governing the whole-system state. Let $p_{S_i}(t)$ denote the probability that the observed system state equals S_i at time t, which can be determined from repeated observations using standard statistical methods. However, inferring component-level hazard rates from $p_{S_i}(t)$ is fundamentally different and necessitates that the system structure be available in a mathematical form. This allows system-level information to be rationally propagated back to the component level. To illustrate, consider a system composed of n components whose observable states correspond to the number of failed components, i.e., $S_0, S_1, \ldots, S_n$ (thus $n+1$ observable

states). Given i failed components, the observed state S_i aggregates $\binom{n}{i}$ possible actual configurations S_{ij}. For an arbitrary component m, among these configurations, the number in which component m is failed equals $\binom{n-1}{i-1}$, while the number in which it is functioning equals $\binom{n-1}{i}$. This many-to-one mapping from actual configurations to observable states highlights why the system structure is essential for inverse inference: without it, system-level probabilities cannot be consistently attributed to component-level failure/survival events.

2.1.2. Component-Level Relevant Information

Statistical moments, sub-component data, and inter-component correlation information are commonly encountered sources of relevant information for component reliability inference. Such information may be available from historical tests, acceptance/qualification reports, maintenance records, and so on. This subsection briefly discusses these three categories of component-level relevant information.

1. Component-wise statistical moment

Components in a k-out-of-n system may originate from different production batches and/or manufacturers. As a result, component-level test data collected during manufacturing and maintenance records obtained during service are often available. In many practical cases, these data are summarized as statistical moments. A typical example is the mean time between failures (MTBF) estimated from maintenance logs. In other cases, lifetime test outcomes are available and may be reported through moments such as the sample mean and variance (or other quantiles). These moment-type summaries can be incorporated as constraints or priors in the inverse inference, thereby reducing the admissible space of hazard-rate functions.

2. Sub-component data

Failure evidence can sometimes be traced to the sub-component level. In the pipeline supply system example, each pump is treated as a component; however, condition monitoring may further identify the failure mode/cause at the sub-component level, such as bearing failure or blade-off. This relationship is schematically represented in Figure 2. The figure illustrates how the sub-components (bearing and blade) affect the pump functionality: failure of either alone lead to pump failure.

Although these sub-component details may not be explicitly modeled in a system-level k-out-of-n formulation (where the pump is the unit of analysis), they provide informative, testable evidence and can be incorporated into the inverse inference process. Figure 3 schematically illustrates the relationship between components and their sub-components in a k-out-of-n system.

To utilize such data, sub-component observations must be translated into mathematical constraints at the component level. A key point is that the relationship between a component and its sub-components is generally asymmetric: failure of a sub-component a (e.g., a bearing) may cause failure of the component b (the pump), whereas failure of the component b does not necessarily imply that sub-component a has failed. To handle this relationship, a multi-function modeling framework can be employed [45], where the component reliability is expressed in terms of the reliabilities of multiple functions supported by sub-components. This representation facilitates the systematic use of sub-component data when constraining the component hazard rate.

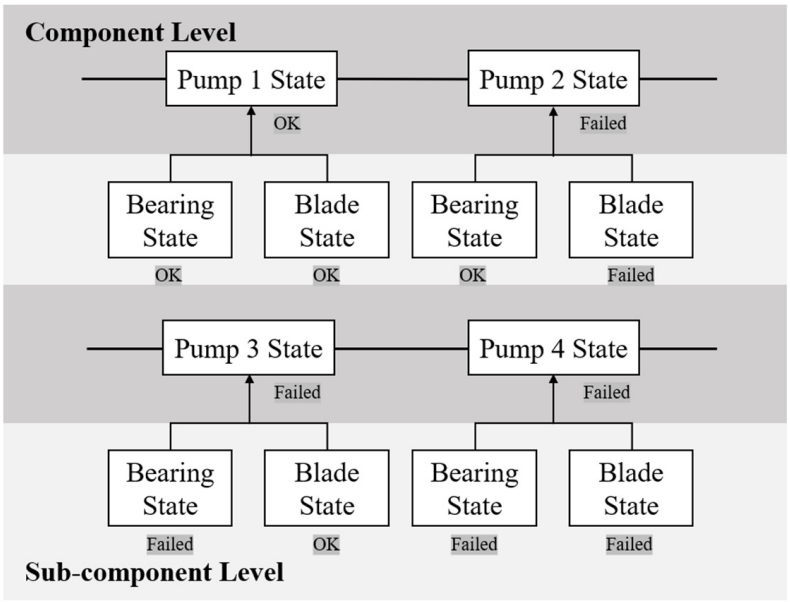

Figure 2. Sub-components and components in the pipeline supply system example.

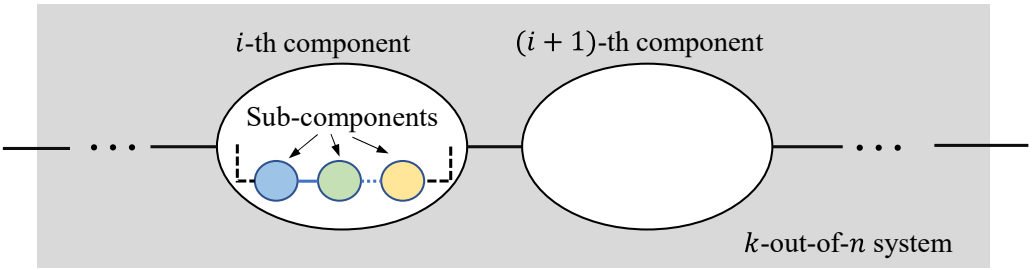

Figure 3. The schematic illustration of the sub-components and components in a k-out-of-n system.

3. Inter-component correlation

Inter-component correlation refers to situations in which the failure of one component can alter the hazard rates of other components. This phenomenon is widely studied in load-sharing models from atomic scale to structural scale [46,47]. In such systems, the failure of a component can cause load redistribution to other components. For example, the failure of one component forces neighboring components to bear increased stress, thereby accelerating their failure. A representative case is the riveted lap-joint structure shown in Figure 4. In this structure, failure of a single rivet triggers immediate load redistribution to the remaining rivets and, consequently, changes their hazard rates. In many applications, the load change induced by a component failure can be estimated analytically or numerically. However, how the hazard rates respond to such changes is highly application-specific. As will be elaborated in Section 2.2, inter-component correlation can be represented through the off-diagonal entries of a hazard-rate matrix [48]. Therefore, correlation information can be used to construct or constrain these off-diagonal terms.

Although Equations (1) and (2) provide a classical reliability expression for k-out-of-n systems, they are not always convenient for systematically incorporating the above types of component-level information, particularly multi-state observations and correlation effects. To facilitate inverse inference under heterogeneous information, the hazard-rate matrix formulation is adopted [48], which provides a unified representation linking system states to component hazard rates.

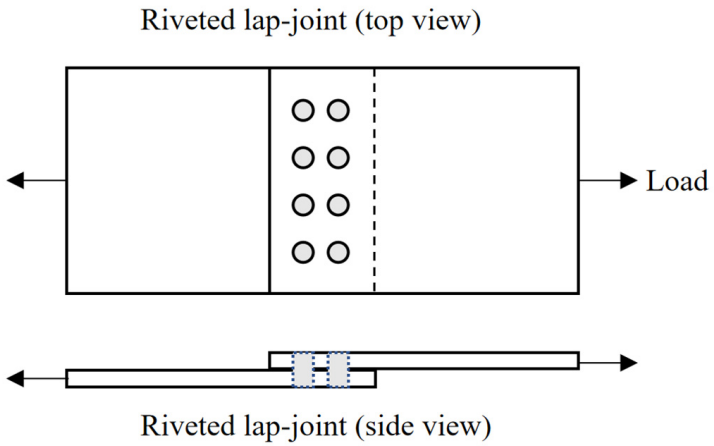

Figure 4. Schematic of a riveted lap-joint structure.

2.2. System Modeling via the Hazard-Rate Matrix

To motivate the discussion, consider a component with an uncertain lifetime T. The reliability (survival) function is defined as $R(t) = \Pr(T \geq t)$ for $t > 0$, and the probability density function (PDF) can be expressed in terms of the reliability function as $p(t) = -\mathrm{d}R(t)/\mathrm{d}t$. The hazard rate function of a component is defined by

$$\lambda(t) \equiv -\frac{1}{R(t)}\frac{\mathrm{d}R(t)}{\mathrm{d}t} = \frac{p(t)}{R(t)}. \tag{4}$$

For a multi-state k-out-of-n system, let $R_i(t)$ denote the reliability that the system is in the i-th state at time t. The reliability functions of the observable states can be written compactly as

$$\frac{\mathrm{d}\mathbf{R}}{\mathrm{d}t} = -\boldsymbol{\lambda}\mathbf{R}, \tag{5}$$

where $\mathbf{R} = [R_1(t), R_2(t), \ldots, R_k(t)]^{T}$ is a column vector composed of $R_i(t)$, $i = 1, 2, \ldots, k$, and $\boldsymbol{\lambda}$ is an n-dimensional upper triangular square matrix,

$$\boldsymbol{\lambda} = \begin{bmatrix} \lambda_{11} & \lambda_{12} & \ldots & \lambda_{1k} \\ 0 & \lambda_{22} & \ldots & \lambda_{2k} \\ \vdots & \vdots & \ddots & \vdots \\ 0 & 0 & \ldots & \lambda_{kk} \end{bmatrix}. \tag{6}$$

The lower triangular entries are set to zero due to the non-increasing property of the reliability function [48].

For functional–structural prior information, suppose prior knowledge indicates a directional relation between two components a and b, denoted by $a \succ b$. Then, the corresponding hazard-rate matrix can be expressed as an upper triangular matrix,

$$\boldsymbol{\lambda} = \begin{bmatrix} \lambda_{aa}(t) & \lambda_{ab}(t) \\ 0 & \lambda_{bb}(t) \end{bmatrix}, \tag{7}$$

where $\lambda_{ab}(t)$ reflects the influence from the failure of component a to component b. In the absence of correlation information, the hazard-rate matrix reduces to a diagonal matrix. For systems with component interactions, $\boldsymbol{\lambda}$ becomes non-diagonal, with off-diagonal entries representing cross-component influences. In the case of mutual influence, $\boldsymbol{\lambda}$ can be modeled as a symmetric matrix. For directional influence, such as in a pipeline system

where upstream pump failures only affect downstream components, $\boldsymbol{\lambda}$ naturally takes a triangular form.

2.3. The Principle of Maximum Entropy

Let f_{ij} denote the conditional probability that the system is in the j-th actual configuration given that a total number of i components have failed. The probability of the system being in a specific state S_{ij} at time t can then be expressed as $p_{S_{ij}}(t) = f_{ij} \cdot p_{S_i}(t)$, where p_{S_i} is the probability that the observed system state is S_i, i.e., exactly i components have failed. The MaxEnt principle is employed to determine the allocated probability f_{ij}, either in the presence or absence of moment data. This approach enables the incorporation of moment information into the inverse information framework for the k-out-of-n system. According to the MaxEnt principle [49], for a given $i \in [0, n]$ and $j \in \left[1, C_n^i\right]$, the entropy associated with the allocated probability f_{ij} is defined as

$$H(f_{ij}) = -\sum_{j=1}^{C_n^i} f_{ij} \log f_{ij}. \tag{8}$$

where f_{ij} is a function of the configuration index j. Given a set of moment data $D = \{\langle d_1 \rangle, \ldots, \langle d_l \rangle, \ldots, \langle d_M \rangle\}$, the moment constraints take the form

$$\sum_{j=1}^{C_n^i} d_l(j) f_{ij} = \langle d_l(j) \rangle, \quad 1 \le l \le M, \tag{9}$$

where M is the number of moment constraints, and $d_l(j)$ represents the l-th moment quantity evaluated at configuration j. Specifically, if the l-th moment quantity corresponds to the mean, then $d_l(j) = j$; if the l-th moment quantity corresponds to the variance, then $d_l(j) = j^2$. To maximize the entropy of Equation (8) subject to the constraints in Equation (9), the following variational condition is required.

$$\delta\left[-\sum_{j=1}^{C_n^i} f_{ij} \log f_{ij} - \sum_{l=1}^{M} \beta_l \left(\sum_{j=1}^{C_n^i} d_l(j) f_{ij} - \langle d_l(j) \rangle\right)\right] = 0. \tag{10}$$

Solving Equation (10) yields the allocated probability f_{ij}

$$f_{ij} = Z^{-1} \exp\left(\sum_{l=1}^{M} -\beta_l d_l(j)\right), \tag{11}$$

where β_l are the Lagrange multipliers determined by

$$\frac{\partial \ln Z}{\partial(-\beta_l)} = \langle d_l(j) \rangle, \tag{12}$$

and the normalization Z is given by

$$Z = \sum_{j=1}^{C_n^i} \exp\left(\sum_{l=1}^{M} -\beta_l d_l(j)\right). \tag{13}$$

In the absence of moment data, the allocated probability f_{ij} reduce to a uniform distribution:

$$f_{ij} = \frac{1}{C_n^i}, \tag{14}$$

which implies that, without additional information, all possible actual configurations S_{ij} are equally likely given that the observed system state is S_i.

3. Inverse Inference Framework for *k*-Out-of-*n* Systems

The inverse inference framework for the *k*-out-of-*n* system is illustrated in Figure 5. Taking observed system state information as input and incorporating additional component-related information as constraints, the allocation probabilities corresponding to different actual system states are computed based on the MaxEnt principle. To support this inverse allocation procedure, the complete enumeration method is adopted to establish an explicit correspondence between system-level states and all admissible component-state configurations. This step is essential because the proposed framework requires the full state-configuration mapping in order to allocate system-level probabilities to latent component states. By contrast, alternative structural analysis methods such as minimal-cut-set or tie-set approaches are generally more suitable for structural reliability evaluation and failure path identification, but they do not directly provide the complete mapping required here, especially when multi-state behavior and auxiliary component information are incorporated. Based on the resulting system–component state correspondence table, component-level failure information can be derived. Building on this framework, the inference process for component-level degradation behavior is discussed in detail for each type of system information introduced above, and the corresponding theoretical solutions are provided.

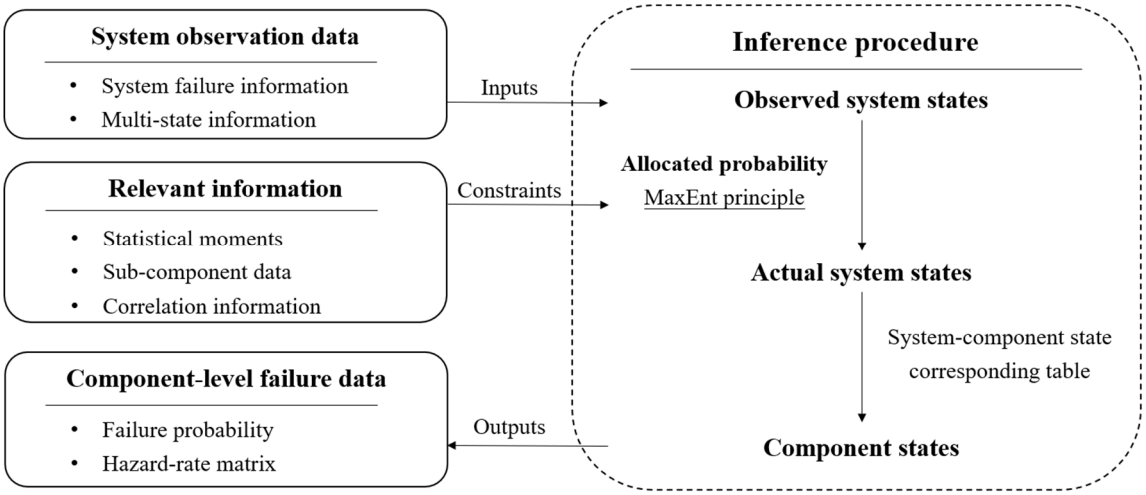

Figure 5. The inverse inference framework for the *k*-out-of-*n* system.

3.1. Inference Using Only System-Level State Observations

Table 1 illustrates the mapping from observable system states (first column) to the underlying component failure configurations in a *k*-out-of-*n* system. To improve readability, the configurations are represented both as binary state vectors and by the associated failed-component sets. In the table, $\mathbb{S} = \{1, q_1, \ldots, q_{k-1}\}$ corresponds to the survival state with probability p_N, and $\mathbb{S} = \{0\}$ corresponds to the failed state with probability p_F.

Table 1. Observable states and corresponding component configurations in a *k*-out-of-*n* system.

$\mathbb{S}$	S_i	S_{ij}	Failed Component Set	Feasible Actual State Configuration
1	S_0	S_{01}	ϕ	(1, 1, …, 1)
q_1	S_1	S_{11}	{1}	(0, 1, …, 1)
		S_{12}	{2}	(1, 0, …, 1)
			⋮	
		$S_{1(C_n^1)}$	$\{n\}$	(1, 1, …, 0)

Table 1. *Cont.*

$\mathbb{S}$	S_i	S_{ij}	Failed Component Set	Feasible Actual State Configuration
⋮	⋮		⋮	
q_{k-1}	S_{k-1}	$S_{(k-1)1}$	$\{1, 2, \ldots, k-1\}$	$(0, 0, \ldots, 1)$
		$S_{(k-1)2}$	$\{1, 2, \ldots, k-2, k\}$	$(0, 0, \ldots, 1)$
			⋮	
		$S_{(k-1)(C_n^{k-1})}$	$\{n-k+2, n-k+3, \ldots, n\}$	$(1, 1, \ldots, 0)$
0	S_k	S_{k1}	$\{1, 2, \ldots, k\}$	$(0, 0, \ldots, 1)$
		S_{k2}	$\{1, 2, \ldots, k-1, k+1\}$	$(0, 0, \ldots, 1)$
			⋮	
		$S_{k(C_n^k)}$	$\{n-k+1, n-k+2, \ldots, n\}$	$(1, 1, \ldots, 0)$
	$S_{k+1}, \ldots, S_n$	...	...	...

In engineering applications of k-out-of-n systems, system states are typically inspected at regular intervals, and multiple lifetime samples $\{t_N\}$ are recorded. The empirical distribution of $\{t_N\}$ is used to estimate the probability p_N of the system being in a survival system state. If monitoring stops once failure occurs, then p_F is not observed. If monitoring continues after failure, additional samples $\{t_F\}$ can be collected to estimate p_F. Without any additional component-relevant information, the probabilities of the actual system states consistent with an observed state are allocated uniformly according to the MaxEnt principle in Section 2.3. Specifically, in the case where the observed system state indicates that a total of i components have failed (with $0 \le i \le n$), there are C_n^i feasible actual states $\{S_{ij}\}_{j=1}^{C_n^i}$. Under uniform allocation, the probability of an actual state S_{ij} is

$$p_{S_{ij}}(t) = \begin{cases} \frac{p_N(t)}{\sum_{i=0}^{k-1}(C_n^i)}, & 0 \le i < k \\ \frac{p_F(t)}{\sum_{i=k}^{n}(C_n^i)}, & k \le i \le n \end{cases}. \tag{15}$$

Let component m be an arbitrary component in the system. For a given i, the number of actual states in which component m has failed equals C_{n-1}^{i-1}. Collecting data on actual system states corresponding to the failure of component m, the failure probability p_m of component m in a k-out-of-n system is expressed as

$$p_m(t) = \sum_{i=0}^{k-1} p_N(t) \frac{C_{n-1}^{i-1}}{C_n^i} + \sum_{i=k}^{n} p_F(t) \frac{C_{n-1}^{i-1}}{C_n^i}. \tag{16}$$

Accordingly, the hazard rate of component m is estimated as

$$\lambda_{mm}(t) = \frac{p_m(t)}{\int_0^t p_m(t')\mathrm{d}t'} = \frac{\sum_{i=0}^{k-1} p_N(t) \frac{C_{n-1}^{i-1}}{C_n^i} + \sum_{i=k}^{n} p_F(t) \frac{C_{n-1}^{i-1}}{C_n^i}}{\int_0^t \left[\sum_{i=0}^{k-1} p_N(t') \frac{C_{n-1}^{i-1}}{C_n^i} + \sum_{i=k}^{n} p_F(t') \frac{C_{n-1}^{i-1}}{C_n^i}\right] \mathrm{d}t'}. \tag{17}$$

The hazard-rate matrix $\boldsymbol{\lambda}$ is an n-dimension square matrix whose diagonal entries are λ_{mm}. In the absence of inter-component dependence information, components are assumed independent and all off-diagonal entries are set to zero, i.e., $\lambda_{mn} = 0$ for $m \neq n$. Because Equations (16) and (17) depend only on system-level observation data and involve no component-specific evidence, the inferred degradation behaviors of all components are identical when only system-level data are available.

For general multi-state monitoring, the system state S_i is observed over time. Let $p_{S_i}(t)$ denote the probability of observing state S_i at time t, estimated from multiple sets of monitoring data. Each observed state S_i corresponds to a set of C_n^i actual states S_{ij}, and their probabilities are related by

$$p_{S_{ij}}(t) = f_{ij} \cdot p_{S_i}(t), \tag{18}$$

where f_{ij} is the allocation weight, i.e., the conditional probability of being in the j-th actual state given a total number of i failed components. Without additional constraints, MaxEnt yields the uniform allocation $f_{ij} = \frac{1}{C_n^i}$. Based on Table 1, consider the set of actual states in which component m has failed. For a fixed number of failed components i, this set contains C_{n-1}^{i-1} states. The failure probability of component m can be written as

$$p_m(t) = \sum_{i=0}^{n} \sum_{j=1}^{C_{n-1}^{i-1}} p_{S_{ij}}(t) = \sum_{i=0}^{n} \sum_{j=1}^{C_{n-1}^{i-1}} \left(\frac{p_{S_i}(t)}{C_n^i} \right). \tag{19}$$

The corresponding diagonal hazard rate is then expressed as

$$\lambda_{mm}(t) = \frac{p_m(t)}{\int_0^t p_m(t')\mathrm{d}t'} = \frac{\sum_{i=0}^{n} \sum_{j=1}^{C_{n-1}^{i-1}} \frac{p_{S_i}(t)}{C_n^i}}{\int_0^t \sum_{i=0}^{n} \sum_{j=1}^{C_{n-1}^{i-1}} \frac{p_{S_i}(t')}{C_n^i} \mathrm{d}t'}. \tag{20}$$

Again, without dependence information, the hazard-rate matrix $\boldsymbol{\lambda}$ is diagonal. Since $p_{S_i}(t)$ contains no component-specific evidence, the inferred diagonal entries are identical across components when only multi-state system-level observations are used.

3.2. Inference with Additional Component-Relevant Information

3.2.1. Incorporating Statistical Moment Information

Building on the multi-state observation data, the inverse inference framework incorporates statistical moment information through the MaxEnt principle introduced in Section 2.3. The system-level observation consists of the multi-state probabilities $p_{S_i}(t)$ for $0 \leq i \leq n$. As established in Section 3.1, each observed state S_i correspond to C_n^i feasible actual states $\{S_{ij}\}_{j=1}^{C_n^i}$, and the probability $p_{S_{ij}}$ of an actual state S_{ij} is expressed as Equation (18). Assume that M moment constraints are available, denoted by $D = \{\langle d_1 \rangle, \ldots, \langle d_l \rangle, \ldots, \langle d_M \rangle\}$. Given exactly i failed components, maximizing the entropy of the allocation probability f_{ij} under the moment constraints based on Equations (8) and (9) leads to the probability of the system residing in the actual state S_{ij}, which is rewritten as

$$p_{S_{ij}}(t) = f_{ij} \cdot p_{S_i}(t) = Z^{-1} \exp\left(\sum_{l=1}^{M} -\beta_l d_l(j) \right) \cdot p_{S_i}(t). \tag{21}$$

Let $p_m(t)$ denote the failure probability of component m. For a given i, there are C_{n-1}^{i-1} actual states in which component m is failed; therefore,

$$p_m(t) = \sum_{i=0}^{n} \sum_{j=1}^{C_{n-1}^{i-1}} p_{S_{ij}}(t) = \sum_{i=0}^{n} \sum_{j=1}^{C_{n-1}^{i-1}} \left[Z^{-1} \exp\left(\sum_{l=1}^{M} -\beta_l d_l(j) \right) \cdot p_{S_i}(t) \right]. \tag{22}$$

Based on Equation (4), the corresponding diagonal hazard rate is determined as

$$\lambda_{mm}(t) = \frac{p_m(t)}{\int_0^t p_m(t')\mathrm{d}t'} = \frac{\sum_{i=0}^{n} \sum_{j=1}^{C_{n-1}^{i-1}} \left[Z^{-1} \exp(\sum_{l=1}^{M} -\beta_l d_l(j)) \cdot p_{S_i}(t) \right]}{\int_0^t \left(\sum_{i=0}^{n} \sum_{j=1}^{C_{n-1}^{i-1}} \left[Z^{-1} \exp(\sum_{l=1}^{M} -\beta_l d_l(j)) \cdot p_{S_i}(t\prime) \right] \right) \mathrm{d}t'}. \tag{23}$$

The hazard-rate matrix $\boldsymbol{\lambda}$ remains diagonal because no inter-component dependence information is given. However, the moment constraints affect the multipliers β_l and thus produce a non-uniform allocation f_{ij}, which leads to distinct inferred diagonal entries $\lambda_{mm}(t)$ across components (in contrast to Section 3.1). In practice, moment information may be reported for variables that are not directly indexed by the system state S_i. In such cases, the moment data must first be transformed into constraints that can be imposed on f_{ij}, i.e., constraints of the form in Equation (9). The resulting component-level degradation behavior is then inferred via Equation (23). A detailed implementation is provided in the numerical examples in Section 4.2.1.

3.2.2. Incorporating Sub-Component Data

This section considers the sub-component data. To leverage such data, the system structure must first be specified so that the sub-component observations can be mapped to the corresponding functional relationships. The physical system is abstracted into a functional system. Consider pump m, which consists of a bearing m_p and a blade m_q. The functions m_p, m_q and m correspond to the survival states of the bearing, the blade, and the pump, respectively. The bearing and blade are assumed to be independent of each other, and both are critical to pump operation. A failure of either the bearing or the blade causes the pump to fail; however, observing a pump failure does not necessarily identify which sub-component has failed. Following the treatment of sub-component data in Section 2.1.2, pump m is treated as a sub-system. Based on the multi-function system degradation reconstruction method, the hazard-rate matrix associated with sub-system m is written as

$$\boldsymbol{\lambda}_{mm} = \begin{bmatrix} \lambda_{m_p m_p} & 0 & \lambda_{m_p m} \\ 0 & \lambda_{m_q m_q} & \lambda_{m_q m} \\ 0 & 0 & \lambda_{mm} \end{bmatrix}, \tag{24}$$

where $\lambda_{m_p m_p}$, $\lambda_{m_q m_q}$ and λ_{mm} are the hazard rates of the bearing, blade, and pump, respectively, and $\lambda_{m_p m}$ and $\lambda_{m_q m}$ quantify the influence of sub-component failures on the pump m. As the bearing and blade affect the pump through the same structural relationship, the bearing–pump pair is used to illustrate the derivation. The structural relation is given by $m_p \succ m$. Given that the pump cannot survive when the bearing has failed, the functional pair (m_p, m) has three possible states, $\{(1,1),(1,0),(0,0)\}$, which are indexed as states 1, 2, and 3, respectively. The degradation evolution is represented by state-transition paths. In this setting, two paths are admissible: $\{123, 13\}$. The sequential path $\{123\}$ is treated as the normal path and is denoted by subscript N. Accordingly, the inputs from sub-component evidence are the path-wise marginal distributions along the normal

path, namely $p_{N.m_p}$, $p_{N.m}$ and analogously $p_{N.m_q}$ for the blade. Following Ref. [45], the corresponding analytical expressions for the hazard-rate elements are

$$\begin{cases} \lambda_{mm}(t) = \frac{p_m(t)}{1-\int_0^t p_m(t\prime)\mathrm{d}t\prime} \\ \lambda_{m_pm_p}(t) = -\frac{p_{N.m_p}(t)}{\int_0^t p_{N.m_p}(t\prime)-p_{N.m}(t\prime)\mathrm{d}t\prime} \\ \lambda_{m_qm_q}(t) = -\frac{p_{N,m_q}(t)}{\int_0^t p_{N.m_q}(t\prime)-p_{N.m}(t\prime)\mathrm{d}t\prime} \\ \lambda_{m_pm}(t) = \frac{p_{N.m_p}(t)}{1-\int_0^t p_m(t\prime)\mathrm{d}t\prime} + \frac{p_{N.m_p}(t)}{\int_0^t p_{N.m_p}(t\prime)-p_{N.m}(t\prime)\mathrm{d}t\prime} \\ \lambda_{m_qm}(t) = \frac{p_{N.m_q}(t)}{1-\int_0^t p_m(t\prime)\mathrm{d}t\prime} + \frac{p_{N.m_q}(t)}{\int_0^t p_{N.m_q}(t\prime)-p_{N.m}(t\prime)\mathrm{d}t\prime} \end{cases}, \tag{25}$$

where $p_m(t)$ denotes the failure probability of pump m, and $p_{N.k}(t)$ represents the marginal distributions of function k (with k in $\{m, m_p, m_q\}$) along the sequential failure path. The quantity $p_m(t)$ can be obtained from the system-level state allocation, for example, via Equation (19), whereas $p_{N.k}(t)$ is provided directly by the sub-component data. Further details are given in Ref. [45]. For a pipeline system consisting of multiple pumps, the overall hazard-rate matrix can be constructed by embedding the sub-system matrix $\boldsymbol{\lambda}_{mm}$ into the system-level matrix. For example, if pump m is one of the units, the system hazard-rate matrix takes a block-diagonal form:

$$\boldsymbol{\lambda} = \begin{bmatrix} \boldsymbol{\lambda}_{aa} & 0 & 0 & 0 & 0 \\ 0 & \ddots & 0 & 0 & 0 \\ 0 & 0 & \boldsymbol{\lambda}_{mm} & 0 & 0 \\ 0 & 0 & 0 & \ddots & 0 \\ 0 & 0 & 0 & 0 & \boldsymbol{\lambda}_{nn} \end{bmatrix} = \begin{bmatrix} \boldsymbol{\lambda}_{aa} & 0 & 0 & 0 & 0 \\ 0 & \ddots & 0 & 0 & 0 \\ 0 & 0 & \begin{bmatrix} \lambda_{m_pm_p} & 0 & \lambda_{m_pm} \\ 0 & \lambda_{m_qm_q} & \lambda_{m_qm} \\ 0 & 0 & \lambda_{mm} \end{bmatrix} & 0 & 0 \\ 0 & 0 & 0 & \ddots & 0 \\ 0 & 0 & 0 & 0 & \boldsymbol{\lambda}_{nn} \end{bmatrix}. \tag{26}$$

By substituting Equation (25) into Equation (26), the hazard-rate matrix of a multi-structure-level system can be expressed using a combination of system-level observation data and sub-component evidence. This decomposition enables complex systems to be analyzed via multiple sub-systems, which simplifies inference and reduces computational cost.

3.2.3. Incorporating Correlation Information

- Strong correlation

Strong correlation information constrains the admissible actual system states by modifying the system-component state correspondence table. Consequently, the component failure probability must be reevaluated by excluding the states that contradict the given strong correlation relations. Based on Equation (19), the failure probability of component m (with m in $\{1, 2, \ldots, n\}$) is rewritten as

$$p_m(t) = \sum_{i=0}^{n} \sum_{j=1}^{(C_{n-1}^{i-1}-q_i)} \frac{p_{S_i}(t)}{C_n^i}, \tag{27}$$

where q_i denotes the number of removed actual states when a total of i components fail, as implied by the strong correlation information. The corresponding diagonal hazard rate is then given by

$$\lambda_{mm}(t) = \frac{p_m(t)}{\int_0^t p_m(t')\mathrm{d}t'} = \frac{\sum_{i=0}^{n} \sum_{j=1}^{(C_{n-1}^{i-1}-q_i)} \frac{p_{S_i}(t)}{C_n^i}}{\int_0^t \sum_{i=0}^{n} \sum_{j=1}^{(C_{n-1}^{i-1}-q_i)} \frac{p_{S_i}(t\prime)}{C_n^i}\mathrm{d}t'}. \tag{28}$$

- Weak correlation

Weak correlation information is incorporated by introducing non-diagonal elements into the hazard-rate matrix. In practice, weak correlation often appears in heterogeneous forms, for example, qualitative dependency descriptions, coupling indicators, or empirical influence scores, and thus cannot be imposed directly as constraints on the allocated probability f_{ij}. To enable its use in the proposed framework, the given weak correlation information is first mapped to weighted coefficients associated with the actual system states through the system-component state correspondence table. The resulting component-level failure probabilities are aggregated, and the corresponding non-diagonal hazard-rate elements are further determined.

Specifically, let $p_{ml}(t)$ denote the failure probability of component l attributable to the influence from component m. According to Equation (19), it can be expressed as

$$p_{ml}(t) = \sum_{i=0}^{n} \sum\nolimits_{Q_{ml}^i} f_{ij} p_{S_i}(t), \tag{29}$$

where Q_{ml}^i is the set of actual system states in which component m exerts influence on component l under the condition that a total of i components fail. The interaction between components m and l (with m, l in $\{a, b, \ldots, n\}$ and $m \neq l$) is characterized by the non-diagonal hazard-rate element λ_{ml}

$$\lambda_{ml}(t) = \frac{p_{ml}(t)}{\int_0^t p_{ml}(t')\mathrm{d}t'} = \frac{\sum_{i=0}^{n} \sum_{Q_{ml}^i} f_{ij} p_{S_i}(t)}{\int_0^t \sum_{i=0}^{n} \sum_{Q_{ml}^i} f_{ij} p_{S_i}(t\prime)\mathrm{d}t'}. \tag{30}$$

If the weak correlation is mutual, then $\lambda_{ml} = \lambda_{lm}$ and the hazard-rate matrix is symmetric. If only downstream components are affected, then $\lambda_{ml} \neq \lambda_{lm}$ and the hazard-rate matrix takes an upper-triangular form. A detailed implementation is provided in the engineering application in Section 4.2.3.

3.2.4. Algorithmic Summary of the Proposed Inference Framework

To clarify the proposed multilevel inference framework, the overall workflow is summarized as follows, and a schematic summary is provided in Figure 6. For a given observed system-level failure state, all feasible actual system states compatible with that observation are first enumerated. Without auxiliary information, these feasible actual system states are assigned uniform allocation probabilities according to the maximum entropy principle. When moment information on the actual system-state probabilities is available, the corresponding maximum entropy distribution can be obtained directly according to Section 2.3, although such information is often difficult to access in practice. A more practical approach is to assign indices to the components and record the index of the component that fails first in each sample. Based on the sample mean of these indices, the component-level failure probabilities are inferred using the maximum entropy principle. These probabilities are then combined with the system-component state correspondence to determine the probability of each feasible actual system state. Normalization within each

subset of states having the same total number of failed components yields the allocation probabilities f_{ij}.

The framework can be further extended when additional information is available. Sub-component information is incorporated by embedding the sub-component structure into the hazard-rate matrix and computing its entries according to Equation (25) in Section 3.2.2. Dependence information is incorporated by updating the probabilities of the feasible actual system states according to the prescribed dependence relationships, followed by renormalization and hazard-rate calculation using the formulas in Section 3.2.3.

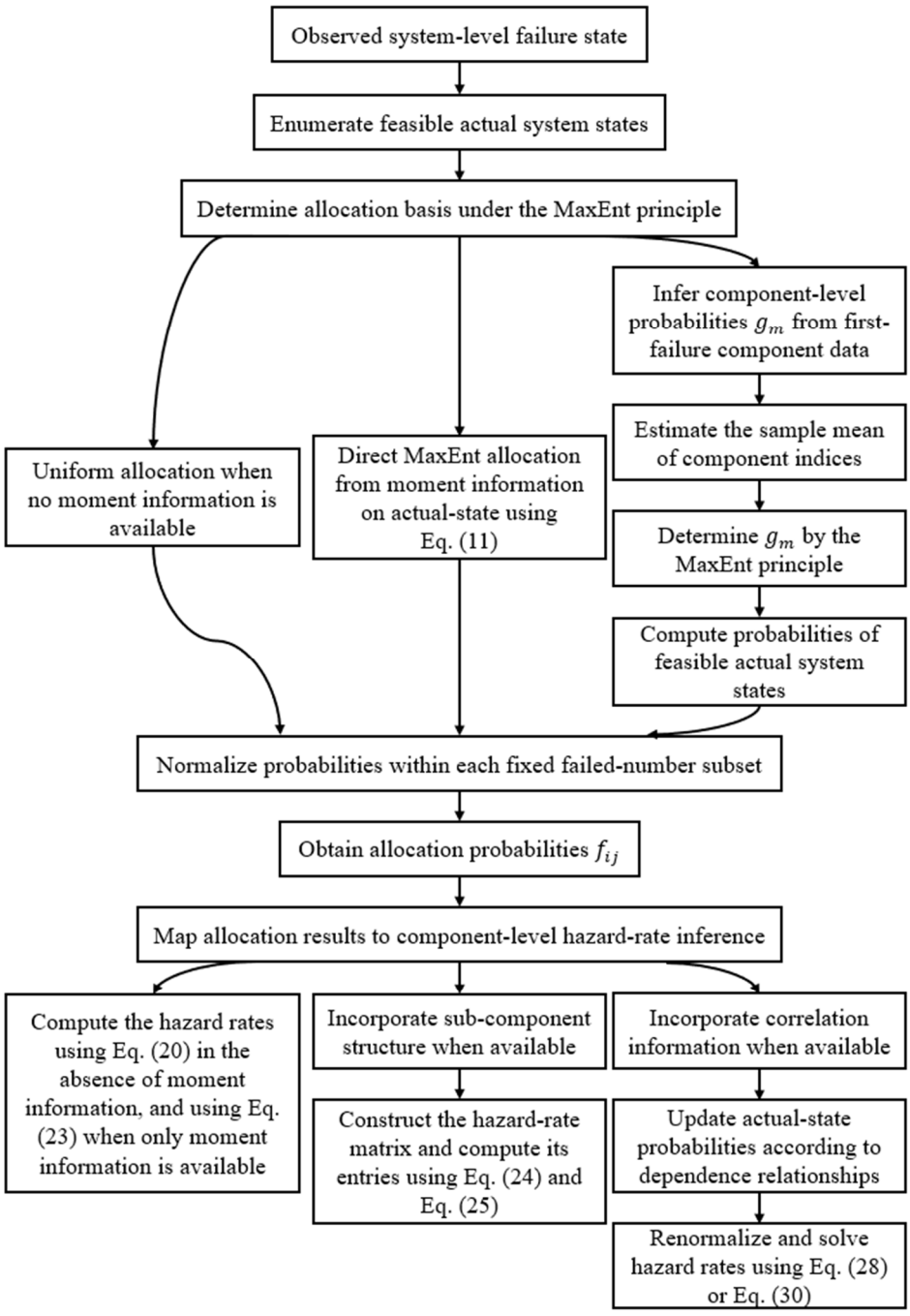

Figure 6. Schematic workflow of the proposed multilevel inference framework.

4. Application to a Long-Distance Pipeline Pumping System

A practical long-distance pipeline transportation system typically employs multiple pumps to ensure continuous delivery and to satisfy operational requirements. During

service, measurement stations are usually installed at regular intervals to monitor system states. In this study, a segment of an operational pipeline between two adjacent measurement points is selected as the research object. The physical configuration of such a pipeline transportation segment is schematically illustrated in Figure 7a, where multiple pumps are deployed within the monitored section. For the specific segment considered in this study, five pumps (pumps *a*, *b*, *c*, *d*, and *e*) are installed between the two adjacent measurement points to jointly support the transport task. According to the operational requirement of the segment, the system is regarded as failed once any two of the five pumps fail. Therefore, the considered pump group is modeled as a two-out-of-five system. The corresponding reliability block diagram is shown in Figure 7b. Figure 7a,b together illustrate the transition from the physical pumping configuration to its reliability representation. The correspondence between system states and component states is summarized in Table 2. The values reported in Table 2 are not directly estimated from component-level field failure statistics; rather, they are inferred allocation probabilities of feasible actual system states based on system-level failure observations and auxiliary information. As the system failure depends on the number of failed pumps rather than on the failure of any specific individual pump, the adopted two-out-of-five formulation is consistent with the general *k*-out-of-*n* framework established in Section 2.

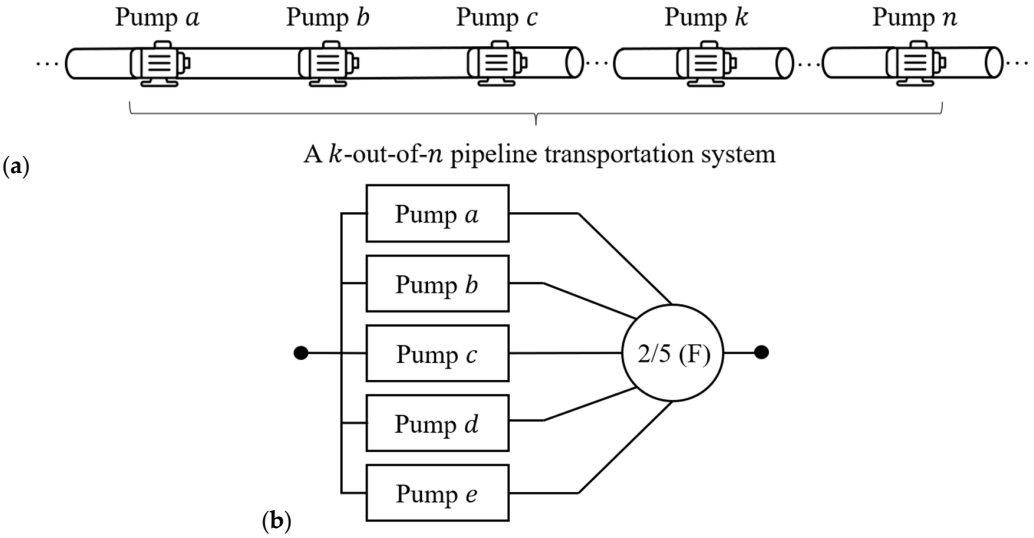

Figure 7. (**a**) A practical pipeline transportation system. (**b**) Reliability block diagram of the case-study pumping system.

Table 2. System-component state correspondence and allocated probabilities.

Observed State S_i	Actual State S_{ij}	Component					Allocated Probability f_{ij}		
		a	*b*	*c*	*d*	*e*(*e*′)	Section 4.2.1	Section 4.2.2	Section 4.2.3
S_0	S_{01}	√	√	√	√	√	1	1	1
S_1	S_{11}	×	√	√	√	√	0.0669	0.0906	0.0815
	S_{12}	√	×	√	√	√	0.1011	0.1368	0.1081
	S_{13}	√	√	×	√	√	0.1560	0.2111	0.1353
	S_{14}	√	√	√	×	√	0.2496	0.3379	0.2121
	S_{15}	√	√	√	√	×	0.4264	0.2237	0.4630

Table 2. *Cont.*

Observed State S_i	Actual State S_{ij}	Component					Allocated Probability f_{ij}		
		a	*b*	*c*	*d*	*e*(*e*′)	Section 4.2.1	Section 4.2.2	Section 4.2.3
S_2	S_{21}	×	×	√	√	√	0.0189	0.0324	0.0316
	S_{22}	×	√	×	√	√	0.0291	0.0500	0.0259
	S_{23}	×	√	√	×	√	0.0466	0.0801	0.0228
	S_{24}	×	√	√	√	×	0.0796	0.0530	0.0487
	S_{25}	√	×	×	√	√	0.0440	0.0755	0.0469
	S_{26}	√	×	√	×	√	0.0704	0.1209	0.0549
	S_{27}	√	×	√	√	×	0.1202	0.0801	0.0575
	S_{28}	√	√	×	×	√	0.1086	0.1866	0.0860
	S_{29}	√	√	×	√	×	0.1856	0.1236	0.1515
	$S_{2(10)}$	√	√	√	×	×	0.2970	0.1978	0.4742
S_3	S_{31}	×	×	×	√	√	0.0182	0.0375	0.0261
	S_{32}	×	×	√	×	√	0.0292	0.0601	0.0139
	S_{33}	×	×	√	√	×	0.0499	0.0398	0.0153
	S_{34}	×	√	×	×	√	0.0451	0.0927	0.0169
	S_{35}	×	√	×	√	×	0.0770	0.0614	0.0313
	S_{36}	×	√	√	×	×	0.1232	0.0983	0.0486
	S_{37}	√	×	×	×	√	0.0680	0.1400	0.0713
	S_{38}	√	×	×	√	×	0.1162	0.0927	0.0362
	S_{39}	√	×	√	×	×	0.1860	0.1484	0.1194
	$S_{3(10)}$	√	√	×	×	×	0.2871	0.2290	0.6209
S_4	S_{41}	×	×	×	×	√	0.0624	0.1465	0.0547
	S_{42}	×	×	×	√	×	0.1065	0.0970	0.0320
	S_{43}	×	×	√	×	×	0.1705	0.1552	0.0355
	S_{44}	×	√	×	×	×	0.2632	0.2396	0.1681
	S_{45}	√	×	×	×	×	0.3974	0.3617	0.7096
S_5	S_{51}	×	×	×	×	×	1	1	1

√ indicates normal operation, × indicates failure.

4.1. System-Level Observations in the Case Study

4.1.1. Inference Using Binary System-State Observations

The considered pipeline segment is modeled as a two-out-of-five system with a binary system state (survival or failure). System state and time information are obtained by monitoring and recording operational observations. From multiple sets of historical records, two time sets $\{t_N\}$ and $\{t_F\}$, corresponding to the survival state and the failed state, respectively, are collected. The probabilities of being in the survival and failed system states are estimated statistically from the observations. In this example, they are assumed to follow

$$p_F(t) = 0.5\mathrm{e}^{-0.5t}, \quad p_N(t) = 0.1\mathrm{e}^{-0.1t}. \tag{31}$$

According to Table 2, the system has $C_5^0 + C_5^1 + C_5^2 = 16$ survival states and $C_5^3 + C_5^4 + C_5^5 = 16$ failed states. Therefore, the probabilities allocated to each actual system states are

$$p_{S_N}(t) = \frac{p_N(t)}{C_5^0+C_5^1+C_5^2}, \quad p_{S_F}(t) = \frac{p_F(t)}{C_5^3+C_5^4+C_5^5}. \tag{32}$$

The component-level failure probabilities and hazard rates are then computed by Equations (16) and (17), and the inferred results are shown in Figure 8. In the absence of additional system-relevant information, the inferred component-level hazard rates are identical for all components. This result reflects the maximum-uncertainty baseline under

the MaxEnt principle, indicating that the proposed inverse framework does not impose artificial distinctions among components when no component-specific evidence is available.

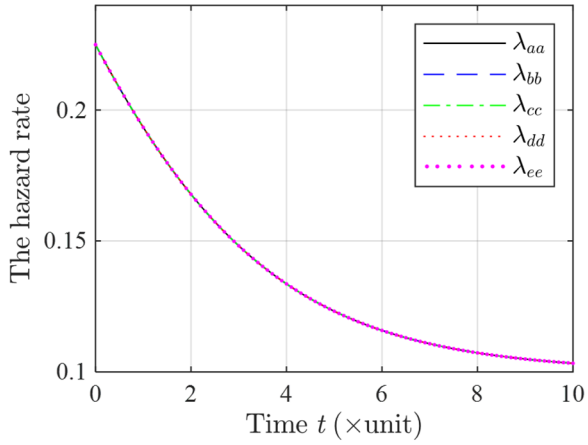

Figure 8. The hazard rates of components inferred by the binary-state failure information.

4.1.2. Inference Using Multi-State System Observations

In engineering practice, measurement stations are equipped with monitoring devices to track the pipeline flow and record the corresponding time data. In this case study, the observed system state is defined based on the port flow level. Specifically, a flow level above 90% indicates that all components survive; a drop to 80%, 70%, 60%, and 50% corresponds to the failure of one, two, three, and four pumps, respectively; and a flow level below 50% indicates that all components fail. Because each observable state corresponds to a specific number of failed components, the observed system state is denoted by S_i, where $i(0 \leq i \leq n)$ is the total number of failed components. Repeating the tests over multiple runs yields the time sets $\{t_i\}$ associated with each state S_i. The probability of being in the observed state S_i, denoted by $p_{S_i}(t)$, is estimated statistically from the recorded observations. In this example, the multi-state observation data are assumed as

$$\begin{cases} p_{S_0}(t) = 0.2\mathrm{e}^{-0.2t} \\ p_{S_1}(t) = 0.15\mathrm{e}^{-0.15t} \\ p_{S_2}(t) = 0.1\mathrm{e}^{-0.1t} \\ p_{S_3}(t) = 0.05\mathrm{e}^{-0.05t} \\ p_{S_4}(t) = 0.025\mathrm{e}^{-0.025t} \\ p_{S_5}(t) = 0.01\mathrm{e}^{-0.01t} \end{cases}. \tag{33}$$

There are C_n^i possible actual system states when a total of i components fail. For the five-pump system, the corresponding numbers are $[1, 5, 10, 10, 5, 1]$ for $i = 0, \ldots, 5$. In the absence of additional system-relevant information, the probability of each actual system state is assumed to be uniformly distributed within the same observed state group, i.e.,

$$p_{S_{ij}}(t) = \frac{p_{S_i}(t)}{C_5^i}, \tag{34}$$

where S_{ij} denotes the j-th actual state among those corresponding to the observed state S_i. Based on Table 2, the component-level failure probabilities and hazard rates are then calculated using Equations (19) and (20), and the inferred results are shown in Figure 9. Since no additional system-relevant information is available, the inferred hazard-rate curves are identical. This again represents the least-informative baseline under the MaxEnt principle, showing that the method preserves structural symmetry and avoids introducing unsupported heterogeneity in the absence of auxiliary information.

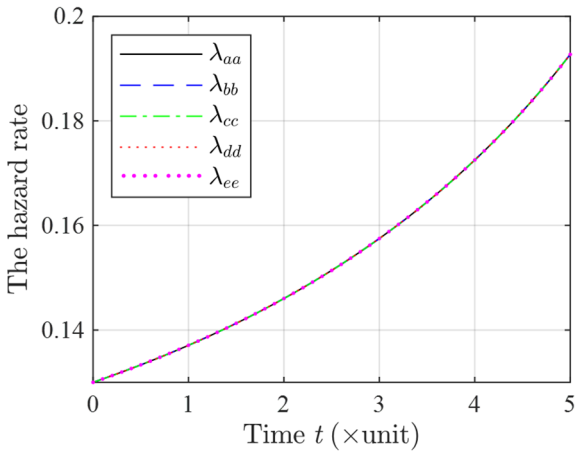

Figure 9. The hazard rates of components inferred by the multi-state failure information.

4.2. Incorporating Component-Relevant Information in the Case Study

4.2.1. Incorporating Testing Moment Data

The system observation data are assumed to be the multi-state information given in Equation (33). In practice, however, moment information directly associated with the true allocation probabilities f_{ij} is generally difficult to obtain. To address this issue, auxiliary component-level information is introduced from development-stage testing of the same type of pipeline system. Specifically, the five pumps (pumps *a*-*e*) are indexed sequentially from 1 to 5. During the tests, the index of each failed pump is recorded, and the sample mean of the failed-pump index is obtained as

$$\sum_{m=1}^{5} m g_m = 3.7, \tag{35}$$

where g_m denotes the failure probability of the m-th component. Based on the MaxEnt principle introduced in Section 2.3, the component failure probabilities are modeled as

$$g_m = Z^{-1}\exp(-\beta m), \quad Z = \sum_{m=1}^{5} \exp(-\beta m). \tag{36}$$

Using the moment-matching condition derived from Equation (12), one obtains $\beta = -0.3704$, and thus $[g_a, g_b, g_c, g_d, g_e] = [0.08346, 0.1209, 0.175, 0.2535, 0.3671]$. As shown in Table 2, each actual system state corresponds uniquely to a specific component-state configuration. Therefore, once the component failure probabilities are obtained, the probability of each actual system state can be constructed accordingly. For example, the probability of state S_{41} is

$$g_{s_{41}} = g_a \times g_b \times g_c \times g_d \times (1 - g_e). \tag{37}$$

Then, for the subset of actual system states associated with a fixed total number of failed pumps, these state probabilities are normalized to obtain the allocation probabilities f_{ij}. The resulting allocations are listed in the third column from the bottom of Table 2. Based on these allocations, the component hazard rates are computed using Equation (23) and are plotted in Figure 10. Since testing-derived component information is incorporated, the inferred component-level degradation behaviors are no longer identical. Although the moment information is extracted from component failure behavior observed under testing conditions, the proposed approach combines such auxiliary component information with practical system monitoring data to infer component degradation behavior in the in-service environment. This result shows that even limited statistical information can break the symmetric baseline and reveal latent heterogeneity among components, thereby

demonstrating the capability of the proposed inverse framework to recover differentiated component-level reliability characteristics from aggregate system-level observations.

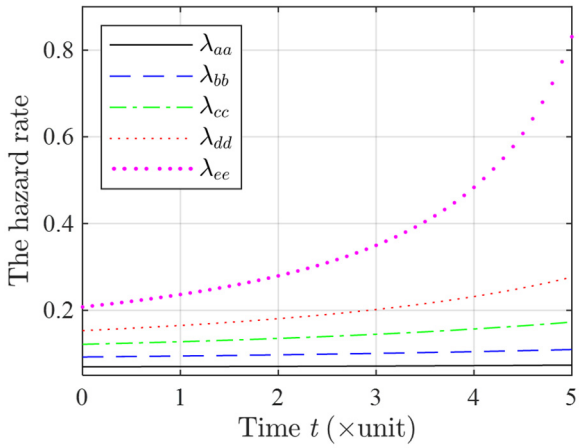

Figure 10. The inferred hazard rates of components with the testing moment data.

4.2.2. Incorporating Maintenance Information

As shown in Section 4.2.1, the inferred hazard rate of pump e is significantly higher than those of the other pumps. To incorporate maintenance information, a maintenance-related enhancement is considered at the fifth pump position by adding a redundant pump, denoted by e', to support pump e. The combined unit formed by e and e' is represented by the equivalent probability associated with the fifth position. For illustrative purposes, this equivalent probability is assumed to be reduced to 50% of the original g_e. The probabilities of the actual system states are then recalculated according to the component-state correspondence in Table 2 and normalized within each subset of states with the same total number of failed pumps, thereby yielding the updated allocation probabilities shown in the second-to-last column of Table 2. The recalculated inferred hazard rates for the components are presented in Figure 11.

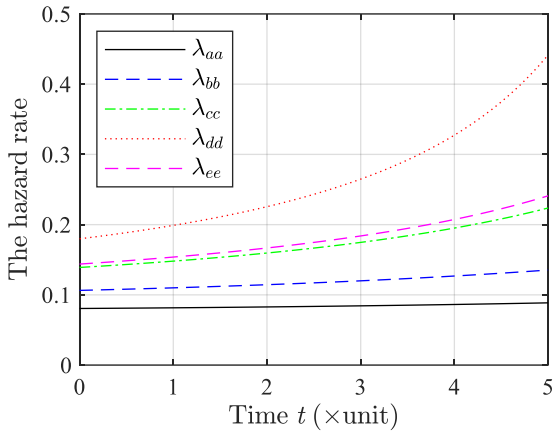

Figure 11. The inferred hazard rates of components with the maintenance information.

After incorporating the maintenance information, the inferred degradation level associated with the fifth pump position becomes markedly lower than that before maintenance, indicating that maintenance enhancement through redundancy can effectively extend the service lifetime of the pipeline system. More importantly, this result demonstrates that maintenance-related information can be explicitly incorporated into the proposed inverse inference framework, thereby reshaping the allocation of component-level failure risk and providing a quantitative basis for evaluating maintenance strategies.

4.2.3. Incorporating Correlation Information

Building on the case setting in Section 4.2.1, mutual dependence among components is further considered. Specifically, the following correlation information is assumed to be available: the failure of one component increases the failure tendency of adjacent components by 50% and that of components two positions away by 30%. Under this correlation setting, the probability of each actual system state is constructed in a state-dependent manner. For a given actual system state, the failed components are first identified, and the failure probabilities of the remaining components are then modified according to their distances from the failed ones. Specifically, if a component m is adjacent to a failed component, its corresponding g_m is multiplied by 1.5; if it is two positions away from a failed component, its g_m is multiplied by 1.3. To ensure probabilistic validity, the modified value is truncated at 1 whenever necessary. Based on these modified component probabilities, the probability associated with each actual system state is calculated through the system-component state correspondence in Table 2. Then, within each subset of actual system states having the same total number of failed components, these state probabilities are normalized to obtain the final allocation probabilities f_{ij}, which are listed in the last column of Table 2. The component-level inference is carried out using Equations (29) and (30), and the results are shown in Figure 12. With mutual correlation, the system hazard-rate matrix becomes a symmetric banded matrix, expressed as

$$\boldsymbol{\lambda} = \begin{bmatrix} \lambda_{aa} & \lambda_{ab} & \lambda_{ac} & 0 & 0 \\ \lambda_{ba} & \lambda_{bb} & \lambda_{bc} & \lambda_{bd} & 0 \\ \lambda_{ca} & \lambda_{cb} & \lambda_{cc} & \lambda_{cd} & \lambda_{ce} \\ 0 & \lambda_{db} & \lambda_{dc} & \lambda_{dd} & \lambda_{de} \\ 0 & 0 & \lambda_{ec} & \lambda_{ed} & \lambda_{ee} \end{bmatrix}. \tag{38}$$

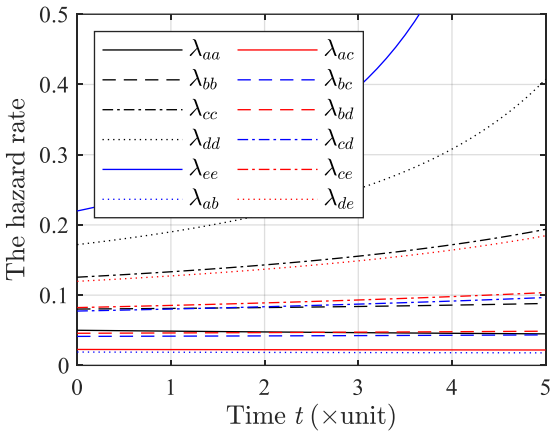

Figure 12. The inferred hazard rates of components with correlation information.

The diagonal entries describe the intrinsic degradation of individual components, whereas the off-diagonal entries quantify the mutual influence between component pairs. Owing to the reciprocal effect between neighboring components, $\boldsymbol{\lambda}$ is symmetric. For clarity, only the upper-triangular entries are visualized in Figure 12. Consequently, the plotted curves are intended to reveal the interaction structure embedded in the system rather than the isolated hazard variation of each individual component. A key insight from this result is that weak dependence changes the representation of degradation from a set of uncoupled component processes to a coupled system-level process. This demonstrates that the proposed framework can explicitly incorporate interaction effects into the inverse reliability inference, thereby providing a richer and more realistic characterization of degradation behavior than models based solely on independent hazards.

Overall, the above results show that the inferred component-level degradation pattern evolves from a uniform baseline to increasingly structured forms as additional information is incorporated. In the absence of auxiliary information, the maximum-entropy inference yields a symmetric reference case in which all feasible actual system states are treated uniformly. Relative to this baseline, the introduction of moment constraints reveals latent heterogeneity among components; maintenance information quantitatively reflects the local reduction in hazard due to intervention; and weak dependence extends the degradation model from independent component-wise hazards to a coupled hazard-rate matrix that captures inter-component interactions. Since no ground-truth component-level hazard rates are available in the present case study, these comparisons are not intended as direct accuracy assessments, but rather as a structured validation of how different sources of auxiliary information progressively enrich the inferred degradation representation and improve its interpretability.

It should also be noted that the present inference framework starts from the empirical distribution of observed system-level failure states and uses maximum-entropy allocation under moment-type constraints, rather than a fully specified component-level prior-likelihood-posterior formulation. Under the available information structure, the no-auxiliary-information case therefore serves as the most natural reference baseline for comparison in this study.

5. Conclusions

This study proposes a theoretical solution to the inverse inference problem for k-out-of-n systems. Existing research on k-out-of-n systems predominantly addresses forward reliability analysis, where component-wise reliability information is assumed to be known and is used to evaluate system reliability. By contrast, the inverse problem considered here aims to rationally transform system-level observation/failure information into component-level reliability information. To this end, the MaxEnt principle is employed to allocate system observation data to actual system states, both in the absence and presence of moment constraints. Based on the correspondence between system states and component-state configurations, component-wise failure information is inferred from the allocated probabilities of the relevant actual system states. The hazard-rate matrix is adopted as a flexible descriptor of component degradation behavior. Within this unified framework, multiple forms of system-level (including multi-state monitoring, testing-derived moments, maintenance actions, and correlation information) can be incorporated consistently for component-level inference. A west-to-east gas pipeline pumping system is used as a case study to demonstrate the applicability of the proposed method in practical engineering settings. The main conclusions are summarized as follows.

- A general MaxEnt-based solution is developed for inverse inference in k-out-of-n system using system-level observation information. The proposed framework establishes a consistent mapping from system-level data to component-level degradation characteristics and provides a unified basis for inverse reliability inference under multiple types of system-level constraints.
- Across four representative information settings, the case study shows that the inferred component-level degradation pattern evolves from a uniform baseline to increasingly structured forms as more informative constraints are incorporated. Specifically, moment information reveals latent heterogeneity, maintenance information reduces the inferred hazard of the protected component, and weak dependence introduces a coupled hazard representation through the hazard-rate matrix.
- The proposed framework provides a consistent way to integrate heterogeneous information sources for inverse inference in k-out-of-n systems. In addition, environmental

effects are implicitly embedded in practical system monitoring data, so no extra preprocessing is required to model such effects explicitly within the proposed inference procedure. This enhances the practical applicability of the method in engineering systems where component-level observations are limited but system-level operational information is available.

- The present study also has limitations. The proposed method relies on full state-space enumeration and may therefore become computationally intensive for large and complex systems. In addition, the inferred component-level results depend on the quality and informativeness of the auxiliary information, including the selected moment constraints, the assumed dependence structure, and the accuracy of the empirical system-state probabilities. A systematic robustness analysis with respect to noisy observations and misspecified auxiliary information is beyond the scope of the present study. Future work will focus on improving computational scalability and robustness under imperfect information, incorporating broader forms of heterogeneous information, and reconstructing system-level failure behavior from the inferred component-level results to achieve a closed-loop inference framework.

Author Contributions: Conceptualization, J.H. and X.G.; methodology, T.G. and D.Z.; software, D.Z.; formal analysis, C.L.; investigation, D.Z.; writing—original draft preparation, C.L., T.G., D.Z. and X.G.; writing—review and editing, C.L., T.G., J.H. and X.G.; visualization, D.Z.; funding acquisition, X.G. All authors have read and agreed to the published version of the manuscript.

Funding: This research was funded by Science Challenge Project, No. TZ2025017.

Data Availability Statement: The original contributions presented in this study are included in the article. Further inquiries can be directed to the corresponding author.

Acknowledgments: The study was supported by Science Challenge Project, No. TZ2025017. The support is gratefully acknowledged. Authors would like to thank the anonymous reviewers for their constructive comments. C. Li and T. Gong contributed equally.

Conflicts of Interest: The authors declare no conflicts of interest.

Abbreviations

n	Number of components in the k-out-of-n system $(n \geq 1)$.
k	Minimum number of components whose failure will lead to failure of the k-out-of-n system $(1 \leq k \leq n)$.
$\mathbb{S}$	The finite set of the observable states of a system, e.g., $\mathbb{S} = \{0, 1\}$ for a binary-state system, and $\mathbb{S} = \{q_c\}$ for a multi-state system, where $0 \leq q_c \leq 1$ is the normalized states, and c is the index of the states.
S_i	The set of states of a k-out-of-n system when a total number of i components fail.
$\lvert S_i \rvert$	The cardinality of the set S_i.
S_{ij}	The j-th n-tuple element of the set S_i.
$R(t)$	Reliability function, survival probability. $R_S(t)$, reliability function of the system. $R_u(t)$, reliability function of the u-th component in the system.
$F(t)$	Failure probability. $F_S(t)$, failure probability of the system. $F_u(t)$, failure probability of the u-th component in the system.
$\Pr(\cdot)$	Probability of an event.
$p(t)$	Probability density function $p(t) = -\frac{\mathrm{d}R(t)}{\mathrm{d}t}$.
$p_{S_i}(t)$	Probability that the system is in state S_i
$p_{S_{ij}}(t)$	Probability that the system is in state S_{ij}
$p_m(t)$	Probability that component m fails
$\lambda(t)$	Hazard rate function $\lambda(t) = \frac{p(t)}{R(t)}$.

λ	Hazard-rate matrix.
f_{ij}	The allocated probability of being in j-th actual state when a total number of i components fail.
T	Lifetime.
H	Entropy about allocated probability f_{ij}, $H\left(f_{ij}\right) = -\sum_{j=1}^{C_n^i} f_{ij}\log f_{ij}$.
D	Moment data set $D = \{\langle d_1\rangle, \ldots, \langle d_l\rangle, \ldots, \langle d_M\rangle\}$.
M	Number of moment constraints.
β	Lagrange multipliers determined by $\frac{\partial \ln Z}{\partial(-\beta_l)} = d_l$.
Z	Normalizing constant.

References

1. Huang, J.; Zuo, M.J. Multi-state k-out-of-n system model and its applications. In *Proceedings of the Annual Reliability and Maintainability Symposium. 2000 Proceedings. International Symposium on Product Quality and Integrity (Cat. No. 00CH37055)*; IEEE: New York, NY, USA, 2000; pp. 264–268. [CrossRef]
2. Birnbaum, Z.W.; Esary, J.D.; Saunders, S.C. Multi-component systems and structures and their reliability. *Technometrics* **1961**, *3*, 55–77. [CrossRef]
3. Kuo, W.; Zhang, W.; Zuo, M. A consecutive-k-out-of-n: G system: The mirror image of a consecutive-k-out-of-n: F system. *IEEE Trans. Reliab.* **1990**, *39*, 244–253. [CrossRef]
4. Boland, P.J.; Proschan, F. The reliability of k out of n systems. *Ann. Probab.* **1983**, *11*, 760–764. [CrossRef]
5. Moore, E.F.; Shannon, C.E. Reliable circuits using less reliable relays. *J. Frankl. Inst.* **1956**, *262*, 191–208. [CrossRef]
6. Von Neumann, J. Probabilistic logics and the synthesis of reliable organisms from unreliable components. *Autom. Stud.* **1956**, *34*, 43–98.
7. Gordon, R. Optimum component redundancy for maximum system reliability. *Oper. Res.* **1957**, *5*, 229–243. [CrossRef]
8. Mine, H. Reliability of a physical system. *IRE Trans. Circuit Theory* **1959**, *6*, 138–151. [CrossRef]
9. Linton, D.G.; Saw, J.G. Reliability analysis of the k-out-of-n: F system. *IEEE Trans. Reliab.* **1974**, *23*, 97–103. [CrossRef]
10. Rykov, V.; Kozyrev, D.; Filimonov, A.; Ivanova, N. On reliability function of a k-out-of-n system with general repair time distribution. *Probab. Eng. Informational Sci.* **2020**, *35*, 885–902. [CrossRef]
11. Ding, Y.; Zuo, M.J.; Tian, Z.; Li, W. The hierarchical weighted multi-state k-out-of-n system model and its application for infrastructure management. *IEEE Trans. Reliab.* **2010**, *59*, 593–603. [CrossRef]
12. Eryilmaz, S. On reliability analysis of a k-out-of-n system with components having random weights. *Reliab. Eng. Syst. Saf.* **2013**, *109*, 41–44. [CrossRef]
13. Sharifi, M.; Taghipour, S. Inspection interval optimization of a weighted-K-out-of-N system with identical multi-state load-sharing components. *Reliab. Eng. Syst. Saf.* **2023**, *238*, 109412. [CrossRef]
14. Wei, C.; Shi, H.; Zhang, Z. Importance measures analysis of two-stage uncertain weighted k-out-of-n systems. *Symmetry* **2025**, *17*, 908. [CrossRef]
15. Coit, D.W.; Chatwattanasiri, N.; Wattanapongsakorn, N.; Konak, A. Dynamic k-out-of-n system reliability with component partnership. *Reliab. Eng. Syst. Saf.* **2015**, *138*, 82–92. [CrossRef]
16. Xie, L.; Zhou, J.; Hao, C. System-level load–strength interference based reliability modeling of k-out-of-n system. *Reliab. Eng. Syst. Saf.* **2004**, *84*, 311–317. [CrossRef]
17. Spaulding, S.L. A Model for Relating Weapons System Availability and Continuous Review Inventory Policies for Repair Parts. Master's Thesis, Naval Postgraduate School, Monterey, CA, USA, 1969.
18. de Smidt-Destombes, K.S.; van der Heijden, M.C.; van Harten, A. On the availability of a k-out-of-N system given limited spares and repair capacity under a condition based maintenance strategy. *Reliab. Eng. Syst. Saf.* **2004**, *83*, 287–300. [CrossRef]
19. de Smidt-Destombes, K.S.; van der Heijden, M.C.; Van Harten, A. On the interaction between maintenance, spare part inventories and repair capacity for a k-out-of-N system with wear-out. *Eur. J. Oper. Res.* **2006**, *174*, 182–200. [CrossRef]
20. Chiang, D.T.; Niu, S.-C. Reliability of consecutive-k-out-of-n: F system. *IEEE Trans. Reliab.* **1981**, *30*, 87–89. [CrossRef]
21. Chao, M.; Fu, J.; Koutras, M. Survey of reliability studies of consecutive-k-out-of-n: F and related systems. *IEEE Trans. Reliab.* **1995**, *44*, 120–127. [CrossRef]
22. Bollinger, R.; Salvia, A. Consecutive-k-out-of-n: F networks. *IEEE Trans. Reliab.* **1982**, *31*, 53–56. [CrossRef]
23. Kossow, A.; Preuss, W. Reliability of consecutive-k-out-of-n: F systems with nonidentical component reliabilities. *IEEE Trans. Reliab.* **1989**, *38*, 229–233. [CrossRef]
24. Yin, J.; Cui, L. Reliability for consecutive-k-out-of-n: F systems with shared components between adjacent subsystems. *Reliab. Eng. Syst. Saf.* **2021**, *210*, 107532. [CrossRef]

25. Fang, S.; Yu, R.; Wu, D.; Peng, R. Reliability of a consecutive *k*-out-of-*n*: *G* system with protection blocks. *Int. J. Gen. Syst.* **2025**, *54*, 421–439. [CrossRef]
26. Lin, M.-S. An O(k_2·log(n)) algorithm for computing the reliability of consecutive-*k*-out-of-*n*: *F* systems. *IEEE Trans. Reliab.* **2004**, *53*, 3–6. [CrossRef]
27. Gökdere, G.; Gürcan, M.; Kılıç, M.B. A new method for computing the reliability of consecutive *k*-out-of-*n*: *F* systems. *Open Phys.* **2016**, *14*, 166–170. [CrossRef]
28. Cluzeau, T.; Keller, J.; Schneeweiss, W. An efficient algorithm for computing the reliability of consecutive-*k*-out-of-*n*: *F* systems. *IEEE Trans. Reliab.* **2008**, *57*, 84–87. [CrossRef]
29. Museli, M. New improved bounds for reliability of consecutive-*k*-out-of-*n*: *F* systems. *J. Appl. Probab.* **2000**, *37*, 1164–1170. [CrossRef]
30. Sarje, A.K.; Prasad, E. An efficient non-recursive algorithm for computing the reliability of *k*-out-of-*n* systems. *IEEE Trans. Reliab.* **1989**, *38*, 234–235. [CrossRef]
31. Shepherd, D.K. k-out-of-n Systems. In *Encyclopedia of Statistics in Quality and Reliability*; John Wiley & Sons, Ltd.: West Sussex, UK, 2008; Volume 2. [CrossRef]
32. Cai, Z.; Si, S.; Sun, S.; Li, C. Optimization of linear consecutive-*k*-out-of-*n* system with a Birnbaum importance-based genetic algorithm. *Reliab. Eng. Syst. Saf.* **2016**, *152*, 248–258. [CrossRef]
33. Davies, K.; Dembińska, A. On the number of failed components in a *k*-out-of-*n* system upon system failure when the lifetimes are discretely distributed. *Reliab. Eng. Syst. Saf.* **2019**, *188*, 47–61. [CrossRef]
34. Petchrompo, S.; Li, H.; Erguido, A.; Riches, C.; Parlikad, A.K. A value-based approach to optimizing long-term maintenance plans for a multi-asset *k*-out-of-*N* system. *Reliab. Eng. Syst. Saf.* **2020**, *200*, 106924. [CrossRef]
35. Singh, A.; Bisht, V.; Singh, S.B. Reliability indices of multi-state repairable *m*-out-of-*r*-within-*k*-out-of-*n* system using L_z-transform method. *Commun. Stat. Theory Methods* **2025**, *54*, 2741–2758. [CrossRef]
36. Roozegar, R.; Nadarrajah, S.; Entezari, M. Reliability properties of k-out-of-n system based on a new mixed δ–shock model. *J. Stat. Theory Pract.* **2025**, *19*, 38. [CrossRef]
37. Ji, D.; Li, W.; Gao, F.; Hua, J.; Lin, J. Adaptive sampling for efficient Lamb wavefield reconstruction in composite laminates with Spatial-Temporal Masked AutoEncoder. *Ultrasonics* **2026**, *162*, 107972. [CrossRef]
38. Yang, J.; Liu, Y.; Lu, X.; Wang, T.; Xie, J.; He, J. Structural response reconstruction based on experimental approximation and model reduction. *Struct. Control Health Monit.* **2026**, *2026*, 5553171. [CrossRef]
39. Liu, H.; Guo, W.; Zhang, J.; Zhu, Y.; He, J.; Guan, X. A curvature-adaptive phased-array synthetic aperture focusing method for flaw detection and size quantification in cylinder-like parts. *Ultrasonics* **2026**, *164*, 108024. [CrossRef] [PubMed]
40. Pan, H.; Hua, J.; Lin, J.; Zhang, Z. Modular and multifunctional phononic-crystal platform for route reconfiguration and information demodulation. *Chin. J. Mech. Eng.* **2025**, 100205. [CrossRef]
41. Li, T.; Lin, Z.; Feng, J.; Wang, Y.; He, J. A maximum entropy moment quadrature method for quasi-real-time flight duration reliability assessment of UAVs. *Reliab. Eng. Syst. Saf.* **2026**, *271*, 112293. [CrossRef]
42. Guan, X. The moment quadrature method for global sensitivity analysis. *Reliab. Eng. Syst. Saf.* **2025**, *265*, 111460. [CrossRef]
43. Gong, T.; He, J.; Guan, X. Continuously nested moment quadrature for uncertainty quantification of black-box models. *Probabilistic Eng. Mech.* **2026**, *83*, 103892. [CrossRef]
44. Jaynes, E.T. Prior probabilities. *IEEE Trans. Syst. Sci. Cybern.* **1968**, *4*, 227–241. [CrossRef]
45. Zhou, D.; Sun, C.; Du, Y.-M.; Guan, X. Degradation and reliability of multi-function systems using the hazard rate matrix and Markovian approximation. *Reliab. Eng. Syst. Saf.* **2021**, *218*, 108166. [CrossRef]
46. Wang, D.; Jiang, C.; Chanseok, P. Reliability analysis of load-sharing systems with memory. *Lifetime Data Anal.* **2019**, *25*, 341–360. [CrossRef] [PubMed]
47. Pérez, R.; Gumbsch, P. An ab initio study of the cleavage anisotropy in silicon. *Acta Mater.* **2000**, *48*, 4517–4530. [CrossRef]
48. Du, Y.-M.; Ma, Y.-H.; Wei, Y.-F.; Guan, X.; Sun, C. Maximum entropy approach to reliability. *Phys. Rev. E* **2020**, *101*, 012106. [CrossRef] [PubMed]
49. Jaynes, E.T. On the rationale of maximum-entropy methods. *Proc. IEEE* **1982**, *70*, 939–952. [CrossRef]